



Faculty of Mechanical Engineering

**VARIABILITY IN VIBRATION INPUT POWER FROM THE
STRUCTURE-BORNE SOUND SOURCE ON PLATE AND BEAM
STRUCTURES**

Noor Fariza binti Saari

Master of Science in Mechanical Engineering

2015

**VARIABILITY IN VIBRATION INPUT POWER FROM THE
STRUCTURE-BORNE SOUND SOURCE ON PLATE AND BEAM STRUCTURES**

NOOR FARIZA BINTI SAARI

**A thesis submitted
in fulfillment of the requirements for the degree of Master of Science
in Mechanical Engineering**

Faculty of Mechanical Engineering

UNIVERSITI TEKNIKAL MALAYSIA MELAKA

2015

DECLARATION

I declare that this thesis entitled, "Variability in vibration input power from the structure-borne sound source on plate and beam structures" is the result of my own research except as cited in the references. The thesis has not been accepted for any degree and is not submitted in candidate of any other degree.

Signature :

Name :

Date :

APPROVAL

I hereby declare that I have read this thesis and in my opinion this thesis is sufficient in terms of scope and quality for the award of Master of Science in Mechanical Engineering

Signature :

Supervisor Name :

Date :

DEDICATION

To my beloved parent, husband, daughter, whole family and friends

ABSTRACT

Structure-borne source which transmits vibration power to the supporting structure especially in buildings plays a major role in contributing structure-borne noise. The structure-borne sources are also capable of causing damage to the receiver structures. In order to prevent noise radiation and structural failure, it is important to characterise the structure-borne sound source and to recognize its potential input power. However, the knowledge of the force excitation behaviors from the structure-borne source which creates variability in the input power is still lacking. To give an effective insight of the structural mechanism excited by the structure-borne source, some uncertainties such as the amplitude, excitation phase and location of the excitation force which create the variability in the input power are modelled in this study. Quantification of the uncertainties of the maximum-minimum bands, frequency-averaged mean and variance are obtained from the variability of input power in the infinite and finite structures. It is shown that the variability of the input power reduces as the frequency increases. It is also found that the quantifications of the variability from the finite structure can also be approached using the infinite structure.

For characterisation of the structure-borne sound source, thin and thick reception structures are used for the velocity source and the force source assumptions in the reception plate test. It is shown that, the reception plate for the force source assumption, the averaging spatial response across the plate area having low modal density is found to be problematic due to high variability of the plate velocity. Therefore, to obtain a more representative spatially averaged mean-squared velocity, only response points closed to the contact points are taken into account in the calculation. The results show that the measured source mobility from the reception plate is improved. Characterisation using a beam structure is also found feasible in the 'reception structure technique'.

ABSTRAK

Sumber bawaan-struktur yang memindahkan kuasa getaran ke struktur sokongan terutamanya di bangunan memainkan peranan utama dalam menyumbang pencemaran bunyi bisu yang disebabkan oleh bawaan-struktur. Sumber getaran oleh struktur mampu menyebabkan kerosakan kepada struktur penerima. Pencirian terhadap sumber bunyi bawaan-struktur dan mengenal pasti potensi kuasa input adalah sangat penting untuk mencegah radiasi bunyi dan kerosakan sesuatu struktur. Walaubagaimanapun, pengetahuan mengenai tingkah laku pengujian daya daripada sumber bawaan-struktur yang mewujudkan kepelbagaian dalam kuasa input masih lagi berkurangan. Untuk memberikan gambaran yang efektif terhadap mekanisma sesuatu struktur, beberapa ketidaktentuan seperti amplitud, fasa pengujian dan kedudukan daya pengujian yang mewujudkan kepelbagaian dalam kuasa input dimodelkan dalam kajian ini. Kuantifikasi jalur maksimum-minimum, purata-frekuensi min dan varians diperolehi daripada kepelbagaian kuasa input dalam struktur terhingga dan tak-terhingga. Didapati bahawa, kepelbagaian kuasa input berkurang semasa frekuensi meningkat. Ianya juga didapati bahawa kuantifikasi daripada struktur terhingga juga boleh diperolehi dan dipadankan dengan menggunakan struktur yang tak-terhingga.

Untuk pencirian sumber bunyi bawaan-struktur, struktur penerima tebal dan nipis digunakan untuk andaian sumber halaju dan sumber daya dalam ujian kaedah plat penerimaan. Ia telah menunjukkan bahawa, dalam kaedah penerimaan plat untuk andaian sumber daya, purata respon ruangan di seluruh kawasan plat yang mempunyai kepadatan modal yang rendah didapati bermasalah disebabkan oleh kepelbagaian halaju plat yang tinggi. Oleh itu, untuk mencari 'min-halaju kuasa dua' yang lebih efektif, hanya pengukuran respon ruangan berhampiran dengan pusat perhubungan (berhampiran motor) diambil dalam pengiraan. Keputusan menunjukkan bahawa mobiliti daripada sumber yang diukur daripada plat penerimaan telah ditambahbaik. Pencirian menggunakan rasuk juga didapati boleh dilakukan dalam ujian 'kaedah penerimaan plat'.

ACKNOWLEDGEMENTS

In the name of Allah, The Beneficent, The Merciful

First and foremost, I would like to give sincere tribute and million thanks to my supervisor, Dr. Azma Putra for his perfect guidance, support and excellent supervision in this research. He never gave up to provide me motivation and optimism throughout this challenging three years. And also thanks to Encik Hairul Bakri and Dr. Reduan Md Dan for their kindness. I would like to also acknowledge the Ministry of Higher Education (MoHE) upon the Fundamental Research Grant Scheme, FRGS/2010/FKM/TK03/15-F00109 for my allowance.

Most importantly, to my beloved husband, daughter, parent and in-laws, thank you so much for your sacrifice and for your ever lasting motivation and support to me especially at the time I felt of losing my hope to finish this study. I am really grateful to have all of you around me. Not also forgotten to all my senior colleagues, Yasser, Sajidin, Munawir, Yusuf and juniors, Farizan, Shyafina, Dayang and others in the Vibro-Acoustics Research Group, I sincerely appreciate your helps, for great discussion and brilliant ideas and those who were very helpful during my study.

My last word, I will always pray all the best for all of you.

TABLE OF CONTENTS

	PAGE
DECLARATION	
APPROVAL	
DEDICATION	
ABSTRACT	i
ABSTRAK	ii
ACKNOWLEDGEMENT	iii
LIST OF FIGURES	vi
LIST OF TABLES	xii
LIST OF ABBREVIATIONS	xiii
LIST OF SYMBOLS	xiv
LIST OF PUBLICATIONS	
CHAPTER	
1 INTRODUCTION	1
1.1 Background	1
1.2 Problem statements	3
1.3 Objectives	4
1.4 Scopes	4
1.5 Thesis outline	5
2 LITERATURE BACKGROUND	7
2.1 Governing mathematical models of vibration input power	7
2.1.1 Input power for single contact point	9
2.1.2 Input power for multiple contact points	10
2.1.3 Quantification of the uncertainty	11
2.2 Past researches on characterising the structure-borne sound sources	13
2.2.1 Velocity source and force source	17
2.2.2 Concept of effective mobility	19
3 METHODOLOGY	21
3.1 Development of mathematical modelling for the vibration input power	21
3.2 Reception structure experiment	23
3.2.1 General equation of reception plate power	24
3.2.2 Measuring squared free velocity	24
3.2.3 Measuring effective source mobility	25
3.2.4 Procedure of reception plate method	26
3.2.4.1 Measuring mobility	28
3.2.4.2 Measuring spatial response	28
3.2.4.3 Direct measurement	30

4	UNCERTAINTY IN VIBRATION INPUT POWER	32
4.1	Variability of input power due to unknown phase in infinite structure	32
4.1.1	Infinite beam structure	32
4.1.1.1	Dependency on the contact points separation	35
4.1.1.2	Random phase	38
4.1.2	Infinite plate structure	40
4.1.2.1	Input power for two point forces	41
4.1.2.2	Input power for four point forces	44
4.2	Variability of input power due to unknown phase in finite structure	48
4.2.1	Finite beam structure	48
4.2.1.1	Input power for a single contact point force	49
4.2.1.2	Averaging over frequency bands	52
4.2.1.3	Averaging over point forcing locations	55
4.2.1.4	Input power for two contact point forces	57
4.2.2	Finite plate structure	61
4.2.2.1	Input power for single contact point force	62
4.2.2.2	Input power for four contact point forces	67
4.3	Summary	69
5	RESULTS OF RECEPTION STRUCTURE EXPERIMENT	71
5.1	Reception plate experiment	71
5.1.1	High mobility reception plate	71
5.1.2	Low mobility reception plate	78
5.2	Reception beam experiment	84
5.2.1	High mobility reception beam	84
5.2.2	Low mobility reception beam	89
5.3	Summary	93
6	CONCLUSION AND RECOMMENDATION	95
6.1	Conclusion	95
6.1.1	The variability of the input power	95
6.1.2	Characterisation on the structure-borne sound source	96
6.2	Thesis contribution	97
6.3	Recommendations	97
	REFERENCES	99

LIST OF FIGURES

FIGURE	TITLE	PAGE
1.1	An illustration of airborne and structure-borne sound transmission path (Source: Author's original work).	2
1.2	Common structure-borne sound sources in buildings (Source: Google's images).	3
2.1	Free velocity and blocked force of a vibrating source.	8
2.2	A source connected to a receiver.	9
2.3	The equivalent source strength using the radiated acoustic space.	13
2.4	The source strength in terms of the free velocity: (a) source and receiver not attached and (b) source is attached to receiver.	14
2.5	The velocity and force sources.	18
3.1	The flowchart diagram of the development mathematical modellings for the uncertainty in vibration input power	22
3.2	The flowchart diagram of the procedure of the reception plate method.	23
3.3	Diagram of the reception plate method.	27
3.4	Diagram of the experimental setup for the reception plate method: mobility measurement on the reception plate.	29
3.5	Measuring the mobility of the source	29
3.6	Diagram of the plate response measurement	30
3.7	Diagram of the direct measurement in term of squared free velocity.	30
4.1	An infinite beam lying in x -axis.	33

4.2	The input power in an infinite beam subjected to a harmonic point force F (Aluminium, $b = 0.03$ m, $h = 0.005$ m; $- \cdot - F = 1$ N, $-- F = 2$ N and $- F = 4$ N).	34
4.3	Illustration of the force contact point separation with respect to the long wavelength for an infinite beam.	36
4.4	Illustration of the force contact point separation with respect to the short wavelength for an infinite beam.	37
4.5	The normalised input power to an infinite beam subjected to two in-phase ($-$) and out-of-phase ($\cdot \cdot \cdot$) harmonic unit point forces	37
4.6	The graph of probability density function Π of the excitation phase.	38
4.7	The input power to an infinite beam subjected to two harmonic point forces with various excitation phases (grey lines): $--$ mean μ , $- \cdot - \mu \pm \sigma$, $\cdot \cdot \cdot$ max/min bounds and $- \mu \pm \sigma$ bounds.	40
4.8	The normalised input power to an infinite plate subjected to two in-phase ($-$) and out-of-phase ($\cdot \cdot \cdot$) harmonic unit point forces and maximum and minimum bounds (thick, grey lines)	42
4.9	The normalised input power to an infinite plate subjected to two harmonic point forces with various relative phases (grey lines): $--$ mean, $- \cdot -$ mean \pm standard deviation, $-$ (thick line) mean \pm bounds of standard deviation, $-$ (thin line) mean \pm bounds of standard deviation due to uncertainty in kL and $\cdot \cdot \cdot$ maximum and minimum bounds of input power.	44
4.10	An infinite plate that excited by four harmonic point forces.	44
4.11	The normalised input power to an infinite plate subjected to four harmonic point forces with various phases (grey lines): $--$ mean, $- \cdot -$ mean \pm standard deviation, $\cdot \cdot \cdot$ mean \pm bounds of standard deviation due to uncertainty in kL , $-$ (thin line) mean \pm bounds of standard deviation, $-$ (thick line) max/min bounds.	47
4.12	Reference of a single point force on the finite beam (Source: Author's original work).	49

4.13	The normalised input power of a finite beam subjected to a single harmonic point force at the middle – and the tip – · – of beam.	50
4.14	The normalised input power to a finite beam subjected to a single harmonic point force for various force locations (grey lines): – actual mean and – · – actual mean \pm standard deviation, (a) $\eta = 0.05$, (b) $\eta = 0.1$.	51
4.15	The normalised input power to a finite beam subjected to a single harmonic point force for various force locations averaged over frequency bands(grey lines): $\eta = 0.05$, – actual mean and – · – actual mean \pm standard deviation.	55
4.16	The averaged mean and standard deviation of the input power of a finite beam with its modal overlap factor; numerical calculation for the finite beam: (–) mean, (– · –) mean \pm standard deviation and; analytical prediction from Eq. (4.51) and Eq. (4.53): (– –) mean, (· · ·) mean \pm standard deviation; ((a) $\eta = 0.05$, (b) $\eta = 0.1$).	57
4.17	A finite beam excited by two point forces.	58
4.18	The normalised input power to a finite beam subjected to two harmonic point forces for various excitation phases (grey lines): $\eta = 0.05$, (–) actual mean and (– · –) actual mean \pm standard deviation.	58
4.19	The normalised input power to a finite beam subjected to two harmonic point forces averaged over all possible excitation phases: $\eta = 0.05$, (–) actual mean and (– · –) actual mean \pm standard deviation.	59
4.20	The relative standard deviation of input power to a finite beam subjected to two harmonic point forces averaged over frequency bands and excitation phases: – finite beam (numerical), – · – infinite beam, – – analytical prediction from Eq. (4.51) and Eq. (4.53) ((a) $\eta = 0.05$, (b) $\eta = 0.1$, (c) $\eta = 0.15$ and (d) $\eta = 0.2$).	60
4.21	Reference of a single point force on the rectangular plate.	62
4.22	The normalised input power to a finite plate subjected to a single harmonic point force ($\eta = 0.5$): (–) middle and (· · ·) tip.	63

4.23	The normalised input power to a finite plate subjected to a single harmonic point force for various force locations (grey lines): (—) actual mean, (— · —) actual mean \pm standard deviation.	64
4.24	The normalised input power to a finite plate subjected to a single harmonic point force for various force locations averaged over frequency bands (grey lines): (—) actual mean, (— · —) actual mean \pm standard deviation.	64
4.25	The averaged mean and standard deviation of the input power of a finite plate with its modal overlap factor; numerical calculation for the finite plate: (—) mean, (— · —) mean \pm standard deviation and; analytical prediction from Eq. (4.51) and Eq. (4.53): (— —) mean, (· · ·) mean \pm standard deviation ((a) $\eta = 0.01$, (b) $\eta = 0.05$, (c) $\eta = 0.1$ and (d) $\eta = 0.15$).	66
4.26	Four contact point forces to a finite plate structure.	67
4.27	The frequency-averaged of normalised input power to a finite plate subjected to four harmonic point forces for various excitation phases: (—) actual mean and (— · —) actual mean \pm standard deviation.	68
4.28	The normalised input power to a finite plate subjected to four harmonic point forces averaged over all possible excitation phases: (—) mean and (— · —) mean \pm standard deviation.	68
4.29	The relative standard deviation of input power to a finite plate subjected to four harmonic point forces averaged over frequency bands and excitation phases: — finite plate (numerical), — · — infinite plate, — — prediction from Eq. (4.51) and Eq. (4.53) ((a) $\eta = 0.05$, (b) $\eta = 0.1$ and (c) $\eta = 0.2$).	70
5.1	The fan motor attached on the high mobility reception plate.	72
5.2	Comparison of measured average mobility from the reception plate (thick solid line) and the fan motor (thin solid line): narrow band (solid line) and one-third octave band (dashed line).	72
5.3	Effective mobility of the high-mobility reception plate assumming: (a) zero phase and (b) random phase.	73
5.4	The measured spatially average mean-squared velocity of the high mobility reception plate (grey line: one-third octave band).	74

5.5	The damping loss factor of the high mobility reception plate.	75
5.6	Measuring the free velocity directly at the feet of the fan motor running at normal speed.	75
5.7	Comparison of the squared free velocity obtained from the reception plate method (thick line) and direct measurement (thin line): (a) zero phase (b) random phase.	77
5.8	The electrical fan motor on the low mobility reception plate.	78
5.9	Comparison of measured average mobility from the reception plate (thick-solid line) and the fan motor (thin-solid line): narrow band (solid line) and one-third octave band (dashed line).	79
5.10	Effective mobility of the source assuming: (a) zero phase and (b) random phase.	80
5.11	Effective mobility of the low mobility reception plate assuming: (a) zero phase and (b) random phase.	80
5.12	Diagram of measurement points for low mobility reception plate.	81
5.13	The measured spatially average mean-squared velocity of the low mobility reception plate: (thick, solid line) the points closed to the motor and (dashed line) all points across the plate.	81
5.14	The damping loss factor of the low mobility reception plate.	82
5.15	Comparison of the source mobility obtained from the reception plate method and direct measurement: (a) zero phase and (b) random phase.	83
5.16	A source connected to a thin receiver beam.	84
5.17	Comparison of measured average mobility from the high mobility reception beam and the fan motor: narrow band (grey, solid line).	85
5.18	Effective mobility of the high mobility reception beam assuming: (a) zero phase and (b) random phase.	86
5.19	The measured spatially average mean-squared velocity of the high mobility reception beam (dashed line: one-third octave band).	86
5.20	The damping loss factor of the high mobility reception beam.	87

5.21	Comparison of the squared free velocity obtained from the reception beam method (grey, thick line) and direct measurement (—): (a) zero phase and (b) random phase.	88
5.22	A source connected to a thick receiver beam.	89
5.23	Comparison of measured average mobility from the low mobility reception beam and the fan motor: narrow band (grey, solid line).	90
5.24	Effective mobility of source by assuming: (a) zero phase and (b) random phase.	90
5.25	Effective mobility of the low mobility reception beam assuming: (a) zero phase and (b) random phase.	91
5.26	Diagram of measurement points for low mobility reception beam.	91
5.27	The measured spatially average mean-squared velocity of the low mobility reception beam (solid line: the points closed to the motor) and (dashed line: all points across the beam).	92
5.28	The damping loss factor of the low mobility reception beam.	92
5.29	Comparison of the source mobility obtained from the reception beam method and direct measurement: (a) zero phase and (b) random phase.	94

LIST OF TABLES

TABLE	TITLE	PAGE
3.1	Material properties for the beam and plate structures.	22
3.2	Dimensions and material for reception plate and beam.	26
3.3	Material properties for reception plate and beam.	27
3.4	List of the equipment used in the experiment.	28

LIST OF ABBREVIATIONS

Hz	Hertz
kHz	kilo Hertz
MOF	Modal Overlap Factor

LIST OF SYMBOLS

a	Length of panel
b	Width of panel
B	Bandwidth
c_L	Longitudinal plate wave speed
E	Young's modulus
F	Force
F_b, f_B	Blocked force
g	Statistical distribution
h	Thickness of panel
$H_n^{(2)}$	Hankel function of the second kind
$i, j = \sqrt{-1}$	Imaginary unit
I	The second mass moment inertia of the structure
k	Acoustic wavenumber
kL	Contact point separation
K_n	n -th order modified Bessel function of the second kind
L	Distance between the contact points
m'	Mass per unit length of panel
m''	Mass per unit area of panel

M	Total mass of panel
n	Number of modes
n_d	Modal density
p, q	Number of natural frequency modes
P_{in}	Input power
\underline{P}_{in}	Minimum input power
\overline{P}_{in}	Maximum input power
Re	Real part
T	Transpose conjugate
v	Velocity
v_f	Free velocity
x_n	Arbitrary n -contact points at x-axis
y_n	Arbitrary n -contact points at y-axis
$Y_i = Y_p$	Input mobility
Y_t	Transfer mobility
$\langle v_R^2 \rangle$	Spatial average of mean-squared velocity
Y_R^Σ, Y_S^Σ	Effective mobility for the receiver and source
z, Z	Impedance
ω	Angular frequency or natural frequency
ρ	Density
η	Damping loss factor
ν	Poisson's ratio

φ	Relative phase
λ	Wavelength
ϕ, θ	Phase
μ	Mean
σ	Standard deviation
Φ	Normalised mode shape

LIST OF PUBLICATIONS

Journal Articles

Putra, A., Saari, N. F., Bakri, H., and Dan, R. M., 2013. Characterisation of structure-borne sound source using reception plate method. *The Scientific World Journal*, Vol.2013, Article ID 742853.

Putra, A., Saari, N. F., Bakri, H., and Ramlan, R., 2014. Vibration strength estimation of a structure-borne source: Case study for a reception beam. *Applied Mechanics and Materials*. Vol. 471(2014), pp. 69-73.

Proceedings

Fariza, N., Putra, A., Bakri, H., and Ramlan, R., 2012. Characterization of a structure-borne source using the reception plate method. *Proceedings of 3rd International Conference on Engineering and ICT*. ICEI 2012, Melaka, Malaysia.

Saari, N.F., Putra, A., Bakri, H., and Md Dan, R., 2015. Variability of vibration input power to a beam structure. *Proceedings of Mechanical Engineering Research Day 2015*, MERD'15, Melaka.

CHAPTER 1

INTRODUCTION

1.1 Background

Noise and vibration in buildings are among the engineering problems need to be solved to provide comfort environment as well as to prevent any unwanted structural damage. Noise in buildings can be divided into two categories based on its transmission path i.e. as airborne and structure-borne noise (Wang, 2010).

The airborne noise is defined when the sound wave generated by a noise source travels through the air and reaches the receiver directly, or it can first reach the wall structure and causes the wall to vibrate and the vibration eventually radiates noise. The noise radiated due to unstable flow from the air conditioning ventilation is the example of the direct airborne noise.

Structure-borne noise however, plays a major part in contributing to the noise pollution in buildings. Most of the noise is often generated by the vibration waves from vibrating and rotating components of mechanical services in buildings. The structure-borne sound originates due to internal force which is acting within a vibrating machine. From the vibrating sources, the vibrational energy is passed to the supporting structure and propagates through the wall, floor and other neighbouring structures in the buildings. Illustration of the airborne and structure-borne noise is shown in Figure 1.1.

The vibration of these structures then causes annoying noise radiation and risks to environment, people's activity and health effect (Flindell and Walker, 2005). Examples of the structure-borne sources in the buildings are fans, compressor, hydraulic equipment, electrical motors, heating pump and washing machines as seen in Figure 1.2.

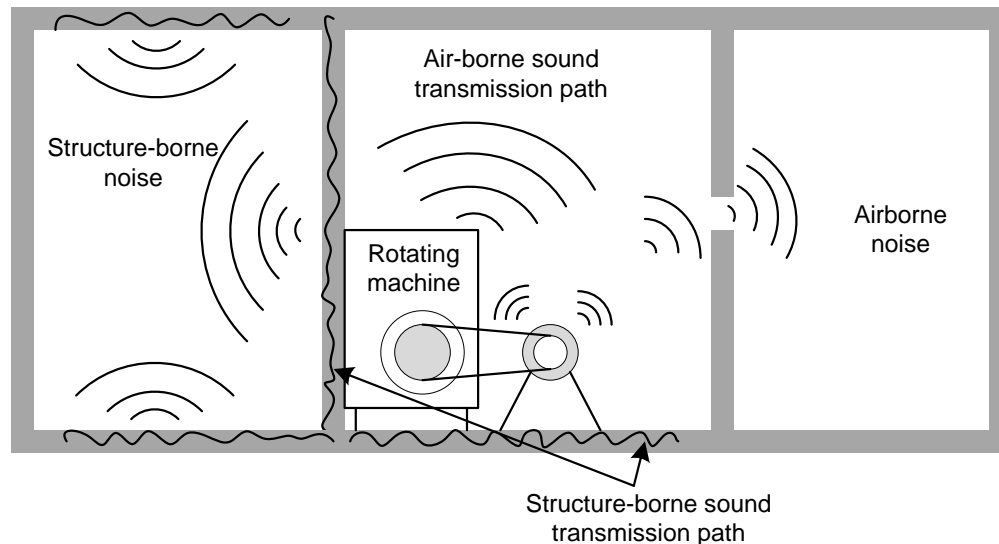


Figure 1.1 An illustration of airborne and structure-borne sound transmission path (Source: Author's original work).

For a long period, the structure-borne sources are capable of injecting high level vibration input power that is hazardous to the receiver structures. The symptoms of structural damage are sometimes not visible and unexpected accident might be occurred due to the lack of knowledge especially the information of input power injected from the machines. Thus, sufficient information about the vibration input power from the structure-borne sound sources is important as a preliminary control measurement. This allows the structural engineers to take a precaution and preventive actions by ensuring the supported structure is strong enough to absorb the potential of the vibration power and also to comply with the acceptable radiated noise levels.